Time-Hopping Sequence Design for Narrowband Interference Suppression

Jason Bellorado[†], Saeed S. Ghassemzadeh[‡], Aleksandar Kavčić[†], Beeta Tarokh[‡‡], and Vahid Tarokh[†]

[†]Harvard University, Division of Engineering and Applied Sciences, Cambridge, MA, USA.

[‡]AT&T Labs-Research, Florham Park, NJ, USA.

[‡‡] Northeastern University, Boston, MA, USA.

***Abstract*— In this paper, we present a simple interference mitigation solution for coexistence of Ultra-Wideband (UWB) systems with other wireless systems. Specifically, we consider the design of *time-hopping* codes for UWB systems that deploy *impulse radio* architecture. We give a methodology for the construction of TH sequences that minimize the imposed UWB interference on a given narrowband system. To illustrate the effectiveness of our designed codes, we conduct physical layer simulations of the interference induced by UWB signals on close proximity wireless local area networks (WLANs) that deploy IEEE 802.11a standard. Our performance measure is the IEEE 802.11a client rate degradation vs. distance from its Access Point. Our results show that, when using optimized TH codes, UWB systems can have no impact on the achievable data-rates and range of IEEE 802.11a WLAN devices; regardless of the position of the UWB system with respect to these devices.**

I. Introduction

On April 22, 2002, the Federal Communication Commission (FCC) issued Ultra-Wideband (UWB) regulations, under Part 15 of the Commission's rules, permitting UWB intentional emissions in the $3100 - 10600$ MHz band subject to radiated power limitations [1]. UWB is defined as any radio technology having a spectrum that occupies a bandwidth greater than 25% of the center frequency or a having a bandwidth in excess of 500 MHz. It is easily construed that, since UWB systems operate in such large and non-dedicated portions of the radio frequency spectrum, they must coexist with a myriad of narrowband and/or broadband radio technologies. For this reason, under Part 15, the UWB indoor intentional emissions are confined to power levels up to -41.3 dBm/MHz in the $3100-10600$ MHz band. This large bandwidth and low power limitation makes UWB an attractive technology for high data-rate, short range, indoor wireless applications [2].

While the FCC mask is said to be sufficient to prevent interference issues, recent studies have shown that UWB signals can significantly affect the operation of underlying narrowband systems [3], [4]. Once such scenario was shown to be when UWB devices operate in close proximity to wireless local area network (WLAN) devices using IEEE 802.11a standard [5]. In [3], the authors show that UWB devices operating at the peak allowable power can significantly impact the achievable data-rate of 802.11a WLAN clients operating in non line-of-sight (NLOS) of their respective Access Points. They also show that 802.11a WLAN devices may induce a significant reduction in the signal-to-interference ratio of a UWB device.

The problem becomes more eminent, namely, how to excise this unavoidable narrowband interference. Methods of narrowband interference excision, such as receiver design [6], directional antennas, notch filters [7] and pulse shaping [8] for wideband systems currently exist. These techniques, while effective, are either complex in receiver design and/or require extensive receiver processing. Multi-banding, proposed in the IEEE 802.15.3a standards [9], is an attractive technique in which the UWB spectrum is divided into many sub-bands. A UWB device, upon detection of the interference in one or multiple sub-bands, stops transmission in those bands, thereby reducing the possibility of interference. All of these techniques have been studied extensively and, thus, are not considered in this work. Here, we consider the task of suppressing UWB interference into a given narrowband victim receiver.

In this paper, we consider generating a UWB signal commonly referred to as *Impulse Radio* (IR) [10]. IR utilizes a train of short-duration pulses to produce a low duty-cycle signal with a spectral density of up to several GHz. The IR transmitter requires a *time-hopping* (TH) sequence (*time-hopping* code) to suppress multiple-access interference [11]. In practice, the TH code must be a finite-length pseudo-random sequence that the transmitter and receiver agree upon prior to transmission and, thus, the actual sequence employed will determine the power spectral density (PSD) of the transmitted signal. We present a design method for generation of TH codes such that the PSD is fully suppressed inside the victim receiver's operating band.

The remainder of this paper is organized as follows: in Section II we define the IR transmit signal, its pulse shape and PSD. In Section III, we discuss the methodology for the design of TH sequences and our optimization results. Section IV details the results of coexistence simulations, followed by a conclusion in Section V.

II. Time-Hopping Impulse Radio Transmitter

A. UWB Signal Definition

Following the convention of [12], we generate a TH-IR signal using a finite-length TH sequence that repeats with a

This material is based upon research supported in part by the National Science Foundation under the grant No. CCR-0118701 and Alan T. Waterman Award, grant No.CCR-0139398.

[†]email:{bellorad,kavcic,vahid}@deas.harvard.edu

[‡]email: saeedg@research.att.com

[‡‡] The author made her contributions to this paper while at AT&T Labs-Research , Florham Park, NJ, USA. email: beeta@coe.neu.edu

repetition period of T_{TH}. The UWB signal, in terms of a single repetition of its TH sequence, is written as

$$x(t) = \sum_{l=0}^{N_b-1} \sum_{h=0}^{N_s-1} a_l \delta\left(t - lT_b - b_l T_\Delta - c_{l,h} T_c - hT_f\right). \quad (1)$$

Here, the TH repetition interval T_{TH} is divided into N_b equal size symbol-intervals of length T_b, each of which corresponding to a modulating data symbol. Each symbol-interval is further divided into N_s frames of length T_f. A single frame contains exactly one pulse, the position of which is dictated both by the TH sequence $\{c_{l,h}\}$ and by the modulating data symbol. The TH sequence adds a pseudo-random delay to each pulse that is equal to an integer multiple of a chip interval T_c. Each frame is divided into N_h chip intervals and, therefore, the TH sequence is a vector of integers from the set $\{0, 1, \ldots, N_h - 1\}$. We refer to the portion of the TH code used to position pulses associated with the l^{th} data symbol as the l^{th} *sub*-TH code (i.e. $(c_{l,0}, c_{l,1}, \ldots, c_{l,N_s-1})$). Thus, a TH code consists of N_b *sub*-TH codes, each of length N_s.

Data is modulated onto the waveform using both Pulse Amplitude Modulation (PAM) and Pulse Position Modulation (PPM), the former of which is represented by the sequence $\{a_l\}$ and the latter by the sequence $\{b_l\}$. An amplitude of a_l, $a_l \in \{1, -1\}$, and a delay of length $b_l T_\Delta$, $b_l \in \{0, 1\}$, is added to the waveform for all pulses that are modulated by the l^{th} data symbol. Note that the defined UWB signal (1) uses a dirac delta function $\delta(\cdot)$ as the pulse shape, however, any pulse may be realized by filtering the signal $x(t)$ using a filter with an impulse response of the desired shape. The transmitted power spectrum is scaled by a multiplicative factor equal to the squared-magnitude of the pulse's Fourier Transform.

Much of the previous work consider a Gaussian monocycle pulse shaping function (first derivative of a Gaussian pulse) for transmission of UWB signals. In [13], it was shown that the lower derivative pulses are non compliant to FCC power mask restrictions. Therefore, we only consider the fourth derivative of a Gaussian pulse, shown in Fig. 1a, which is given by

$$v(t) = \frac{A}{\sqrt{2\pi}\sigma^5} \exp\left(-\frac{t^2}{2\sigma^2}\right)\left(\frac{t^4}{\sigma^4} - \frac{6t^2}{\sigma^2} + 3\right), \quad (2)$$

and has a Fourier Transform (Fig. 1b)

$$V(f) = A(j2\pi f)^4 \exp\left(-\frac{(2\pi f\sigma)^2}{2}\right). \quad (3)$$

The pulse time parameter σ controls the pulse width (99.9% of the power is contained within $[-3.5\sigma, 3.5\sigma]$) and the center frequency f_c of its Fourier Transform ($f_c \approx 1/\pi\sigma$).

B. UWB Power Spectral Density

Assuming that the amplitude $\{a_l\}$ and time-shift $\{b_l\}$ modulation processes are independent, white random processes, uniformly distributed over their respective signal sets, then the PSD of the UWB signal (1) is given in [12] by

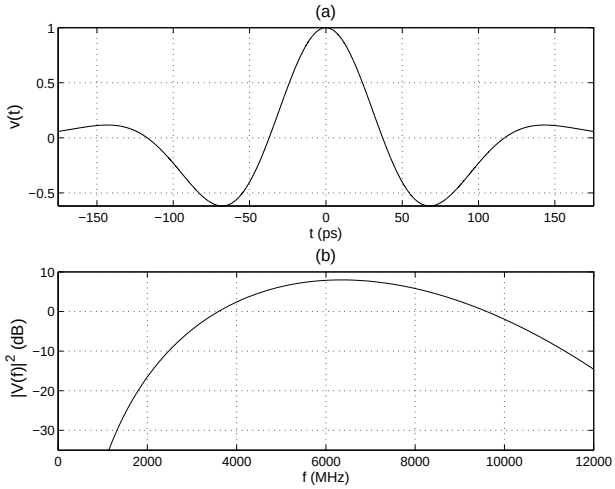

Fig.1: **(a)** Fourth derivative of a Gaussian pulse (see (2)) with time parameter $\sigma = 50.1275$ ps normalized by its peak amplitude. **(b)** Squared magnitude (in dB) of the Fourier Transform of the Fourth derivative of a Gaussian pulse (see (3)) normalized by its median value. The center frequency is given by, $f_c \approx 1/\pi\sigma = 6350$ MHz.

$$P_{xx}(f) = \frac{E\left[a_l^2\right]}{T_{\text{TH}}} \sum_{l=0}^{N_b-1} \left| e^{-j2\pi f l T_b} \sum_{h=0}^{N_s-1} e^{-j2\pi f(c_{l,h}T_c + hT_f)} \right|^2$$
$$= \frac{E\left[a_l^2\right]}{T_{\text{TH}}} \sum_{l=0}^{N_b-1} \sum_{h_1,h_2=0}^{N_s-1} e^{-j2\pi f\left[T_f(h_1-h_2) + T_c\left(c_{l,h_1} - c_{l,h_2}\right)\right]}. \quad (4)$$

Expanding each term of the summation, the imaginary part of the summation may be dropped because each term is a squared-magnitude and, therefore, must be real. The resultant expression for transmitted PSD is given by

$$P_{xx}(f) = \frac{E\left[a_l^2\right]}{T_b N_b} \sum_{l=0}^{N_b-1} \left[\sum_{h_1,h_2=0}^{N_s-1} \cos\left(2\pi f\left[T_f\left(h_1 - h_2\right) + T_c\left(c_{l,h_1} - c_{l,h_2}\right)\right]\right) \right]. \quad (5)$$

We note that the second (bracketed) term in (5) is, up to a positive scaling constant, the transmitted PSD that would result by setting $N_b = 1$ and choosing the TH sequence as the l^{th} *sub*-TH code. We will denote this PSD by $P_{xx}^l(f)$. Thus, by allowing the TH sequence to span more than a single data symbol ($N_b > 1$), the resultant PSD is the average of the N_b power spectral densities, $P_{xx}^l(f)$, $l \in \{0, 1, \ldots, N_b - 1\}$.

The transmitted UWB signal is the convolution of the random *Impulse Radio* waveform (1) with the pulse shape (2). Therefore, the transmitted PSD is given by the PSD of the random waveform scaled by the squared magnitude of the Fourier Transform of the pulse as

$$P_{zz}(f) = |V(f)|^2 \cdot P_{xx}(f)$$
$$= \frac{A^2 E\left[a_l^2\right](2\pi f)^8}{T_b N_b} e^{-(2\pi f\sigma)^2} \times \sum_{l=0}^{N_b-1} \sum_{h_1,h_2=0}^{N_s-1} \cos\left(2\pi f\left[T_f\left(h_1 - h_2\right) + T_c\left(c_{l,h_1} - c_{l,h_2}\right)\right]\right). \quad (6)$$

Although (6) defines the PSD of the transmitted signal, the design procedure detailed in the following section optimizes the PSD expression of (5) to minimize UWB interference into a given narrowband system. This approach is justified because the utilized TH sequence is only capable of changing this part of the PSD. Also, since the effect of the pulse shape is through a multiplicative factor, inducing a spectral *notch* in this part of the PSD will also induce a notch in the transmitted PSD.

III. The Design of UWB Time-Hopping Sequences

Our objective is to develop a TH sequence design method for minimizing the interference by UWB signals onto any device operating in the underlaid spectrum. To narrow our broad objective, we will devise this method for 802.11a WLANs. Bear in mind that, although we are specifically discussing the interference between UWB and 802.11a WLANs, the following design method is applicable to the mitigation of TH-IR UWB interference into any given narrowband system.

A. Time-Hopping Sequence Design

We begin the design procedure by reiterating that the resultant PSD of the UWB signal is the average of the PSDs achieved by using each *sub*-TH code individually. Thus, if there exists a single optimal *sub*-TH code (a code that radiates the smallest percentage of its power into the 802.11a band) then averaging the PSD achieved with this *sub*-TH code with any other PSD can only increase the percentage of the total energy radiated into this band (since a PSD is non-negative for all frequencies). We, thus, assert that choosing $N_b = 1$ is optimal in this respect. We make this assumption and return to the case of $N_b > 1$ later. Note that this assumption drastically reduces the number of codes that may be considered since there exist $N_h^{N_b \cdot N_s}$ valid TH codes. Since we are only considering TH sequences with $N_b = 1$, we drop the first subscript on components of the TH sequence in (5) and give the final expression for this portion of the transmitted PSD as

$$P_{xx}(f)=\frac{E[a_l^2]}{T_b}\sum_{h_1,h_2=0}^{N_s-1}\cos(2\pi f[T_f(h_1-h_2)+T_c(c_{h_1}-c_{h_2})]). \quad (7)$$

Using this expression, we next develop a gradient descent style algorithm for obtaining *good* codes. Although TH codes are chosen from the set $\mathcal{A} = \{0, 1, \ldots, N_h - 1\}^{N_b \cdot N_s}$, we assume that they take on values in $\mathbb{R}^{N_b \cdot N_s}$ and quantize the sequence to $\mathcal{A}$ after convergence. The continuous gradient descent algorithm is, then, given by the following iterative equation:

$$\underline{c}^{(k+1)} = \underline{c}^{(k)} - \eta(k)\nabla J(\underline{c})|_{\underline{c}=\underline{c}^{(k)}}. \quad (8)$$

Here, the TH sequence at iteration k is given by the vector $\underline{c}^{(k)}$, $\nabla J(\underline{c})$ is the gradient of the objective function, and $n(k)$ is the step size. The objective function is the percent of the total UWB power falling inside of the 802.11a band. We base our algorithm on a discretized power spectrum and denote the set of all frequencies (from DC to the sampling frequency) as β, and the set of frequencies inside of the 802.11a band as β'. Thus, objective function is given by

$$J(\underline{c}) = \left[\sum_{f_m \in \beta'} P_{xx}(f_m)\right] \cdot \left[\sum_{f_m \in \beta} P_{xx}(f_m)\right]^{-1}, \quad (9)$$

where $P_{xx}(f_m)$ is given by (7). To obtain a single dimension of the gradient vector, the derivative of (9) with respect to a single element of the TH code is arrived at using the chain rule. The step size $\eta(k)$ in (8) decays logrithmically with k.

As is the case in any gradient descent algorithm, convergence is only guaranteed to a stable point, and not to a global minimum, of the objective function. Thus, by randomizing the starting sequence $\underline{c}^{(0)}$, the algorithm may converge to different, *locally optimal*, TH codes. By carrying out this optimization procedure using randomized starting vectors, it was determined that there exist multiple TH sequences that give very small values of $J(\underline{c}^{(\infty)})$. We may, therefore, construct longer codes by concatenating these *locally optimal sub*-TH codes. These longer codes, due to the averaging property of PSDs, produce signals that maintain the property of radiating a small fraction of their total power into the band of interest, but will have a flatter PSD outside this band. Thus, the algorithm we implemented collects multiple *good sub*-TH sequences and creates longer codes that minimize the out-of-band deviation about the median PSD.

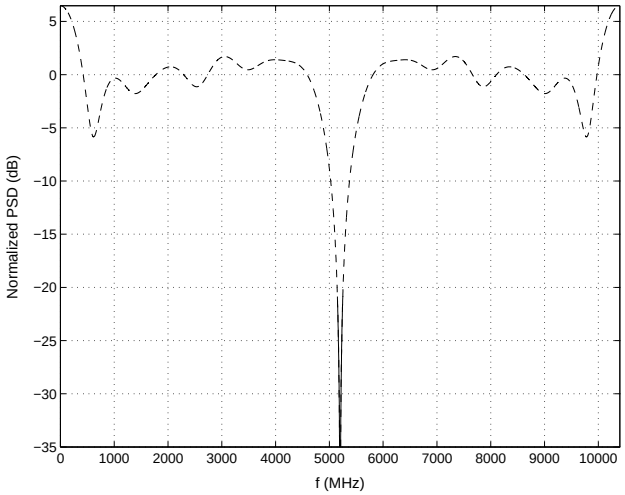

Fig.2: Normalized PSD of a *Time-Hopping Impulse Radio* signal utilizing the optimized TH sequence given in Section IIIb. The portion of the spectrum depicted as a solid line is the UWB PSD that falls inside the lower U-NII frequency band ($5150 - 5250$ MHz).

B. Optimization Results

The optimization procedure developed in the preceding subsection was carried out for the following TH code parameters: $N_b = 7$, $T_b = 1.5384$ ns, $N_s = 4$, $T_f = 384.61$ ps, $N_h = 4$, $T_c = 96.15$ ps. Although we found several codes that produce a signal that radiates a small percentage of its total power into the lower U-NII frequency band ($5150 - 5250$ MHz), the TH sequence given by $[2130, 2330, 0310, 0332, 2121, 1230, 0321]$ produced a PSD with minimum variance about the median (Fig. 2). The PSD depicted in Fig. 2 is that of the random

process defined by (1) and, thus, does not include the pulse shape. As can be seen, the -3 dB frequency band, with respect to the median PSD, is $4804 - 5597$ MHz, giving a -3 dB bandwidth of 793 MHz. The portion of the spectrum inside the lower U-NII frequency band (depicted as a solid line) is over 21 dB below the median PSD throughout the 802.11a band. As the number of *sub*-TH codes is increased (increasing N_b), the width and depth of the notch are reduced. This is mainly due to averaging.

IV. Coexistence Simulations

A. Simulation Parameters

1) The UWB Signal: In our simulations, we assume a pulse with $\sigma = 50.1275$ ps, producing a 350 ps wide pulse with a center frequency of 6350 MHz (Fig. 1). The methodology for choosing σ to produce a signal that is in compliance with the FCC spectral mask is discussed in detail in [13] and, thus, is omitted here.

The pulse amplitude A was adjusted to ensure that the transmitted PSD remained below the in-band spectral mask of -41.3 dBm/MHz in the $3100 - 10600$ MHz frequency band. This requires that the integral of the transmitted PSD over any 1 MHz of spectrum be upper bounded by $10^{(-41.3/10)}$. As shown by (6), A scales the transmitted PSD by its square. Thus, we determined the 1 MHz band into which the UWB signal radiates the most power and chose A such that the spectral mask was met with equality in this band. The resultant PSD is plotted along with the FCC power mask in Fig. 3. The pulse amplitude that produces a signal in compliance with FCC regulations gives a total power of -66.7 dBm.

2) The 802.11a WLAN: A WLAN PHY simulator based on that of [5] operating in the lower U-NII frequency band centered at 5200 MHz was built in Matlab. We consider a WLAN operating at the peak allowable power density in this band of 2.5mW/MHz. We calculate the WLAN receiver noise output power in terms of Boltzman's constant (k) and the ambient temperature (T) [14] as

$$N_{0,802.11a} = 10\log_{10}(kT) + NF_{802.11a} + 10\log_{10}(BW_{802.11a}). \quad (10)$$

Here $NF_{802.11a}$ is the noise figure (6 dB) and $BW_{802.11a}$ is the WLAN receiver bandwidth of 20 MHz. The WLAN receiver noise power is calculated as $N_{0,802.11a} = -95$ dBm.

3) The Propagation Medium:

a) UWB Channel Model: In [15] the path loss model is given for an indoor environment as

$$PL(d) = PL_0 + 10\gamma\log_{10}(d) + S \quad (\text{dB}). \quad (11)$$

PL_0 is the median path loss at 1 meter, which was determined experimentally to be 47 dB and 51 dB for LOS and NLOS environments, respectively. The constant γ defines the slope of the path loss (on a dB scale) and was determined empirically to be 1.7 in for LOS paths and 3.5 for NLOS paths. The effect of shadow fading [14] is modeled by the zero-mean Gaussian random variable S with standard deviation of 2.8 dB for LOS paths and 3.8 dB for NLOS paths (see [15]).

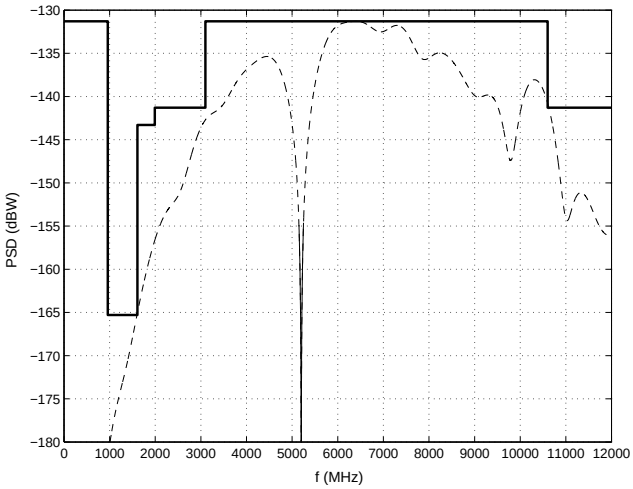

Fig.3: Transmitted UWB PSD utilizing the optimized TH sequence (see Section IIIb) and pulse shape parameters discussed in Section IVa-1. The PSD mask defined by the FCC for UWB transmission is shown as a thick solid line. The portion of the spectrum depicted as a solid line is the UWB PSD that falls inside the lower U-NII frequency band ($5150 - 5250$ MHz).

b) WLAN Channel Model: We assume a Ricean flat-fading channel with a K-factor of 6 dB for LOS paths and a Rayleigh flat-fading channel was for NLOS paths [14]. Since the median path loss of a signal is independent of its bandwidth, we use the same path loss model given by (11) for the WLAN signal.

c) Received Power Calculation: We use (11) to calculate the power collected by a receiver from a signal propagating over a distance of d meters. Denoting the total power of the transmitted signal in the frequency range $[f_1, f_2]$ by $P(f_1, f_2)$, we calculate the received power as

$$P_R = P(f_1, f_2) - PL(d), \quad (12)$$

where f_1 and f_2 are the lower and upper band-edges, respectively, of the receiver.

B. Simulation Results

The results of interference simulations given in [3] showed that UWB induces the greatest impact on the achievable rate of an 802.11a WLAN when it is operating in LOS of the victim receiver, while the WLAN is operating in NLOS. Therefore, we only consider the LOS case.

To analyze the performance of our proposed TH sequences, we first consider a UWB signal employing a TH code selected uniformly-at-random from all valid TH codes with parameters given in Section IIIb. We note that, although the interference resulting from this signal is dependent upon the actual TH code employed, numerous simulations have shown that the interference presented is representative of the majority of valid TH sequences. The resultant UWB signal has total power of -66.8 dBm, where -91.6 dBm falls into the U-NII frequency band centered at 5200 MHz. The maximum power that UWB may radiate in this band is -88.3 dBm. The achievable data-rate of an 802.11a WLAN operating in UWB interference is shown in Fig. 4. With the UWB transmitter at a distance of 1m from the WLAN receiver, the WLAN can only support

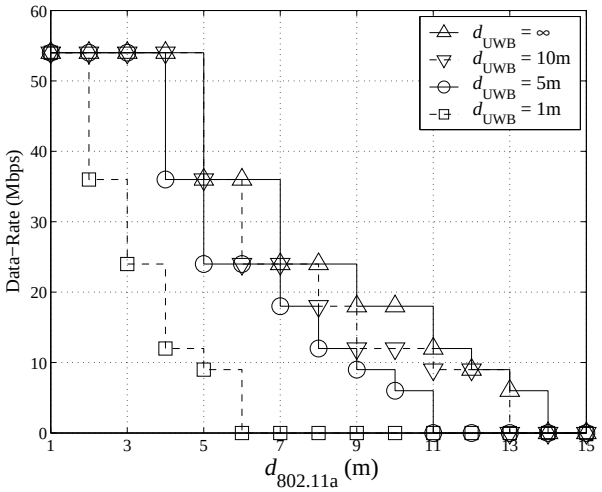

Fig.4: Achievable data-rate of an 802.11a WLAN operating with a T-R separation of $d_{802.11a}$ with no LOS between transmitter and receiver. The UWB interferer is within LOS of the WLAN receiver at a distance of d_{UWB} and is employing a random TH code. Note that, as specified by the 802.11a standard, only data-rates of 54, 48, 36, 24, 12, 9, and 6 Mbps are supported.

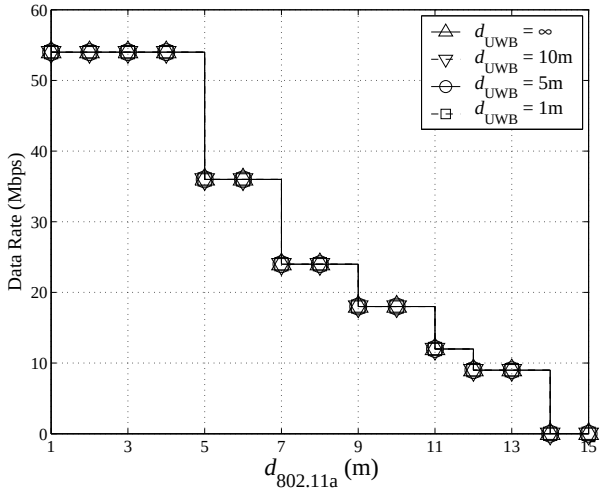

Fig.5: Achievable data-rate of an 802.11a WLAN operating with a T-R separation of $d_{802.11a}$ with no LOS between transmitter and receiver. The UWB interferer is within LOS of the WLAN receiver at a distance of d_{UWB} and is employing the optimized TH code specified in Section IIIb. For all scenarios considered there is no loss in achievable rate in the presence of UWB interference as compared to the no-interference case.

24 Mbps at a transmitter-receiver (T-R) separation of 3m (54 Mbps is supported at this distance without UWB interference) and the WLAN is completely jammed for a T-R separation in excess of 5m. When the UWB interferer is a distance of 5m and 10m from the WLAN receiver, the loss in achievable rate is shown to be as large as 18 and 12 Mbps, respectively.

When employing the optimized TH sequence (Section IIIb) the pulse amplitude chosen to comply with FCC regulations gives a transmitted power of -66.7 dBm. However, the notch induced by the TH code in the transmitted PSD (Fig. 3) gives a total power radiated into the 802.11a band of -130.4 dBm, $.013\%$ of the in-band power radiated using a random TH sequence. Using the equivalent simulation as completed for a random TH code, we have shown that the 802.11a WLAN exhibited no loss in achievable data-rate over the case of no UWB interference (Fig. 5). We note that, since we are considering the most difficult case of WLAN transmission (i.e. the WLAN operating in NLOS and the interferer within LOS of the victim receiver), the designed TH code will suppress UWB interference for all transmitter/interferer setups.

V. Conclusion

In this paper, we explored the design and optimization of TH codes to suppress the interference imposed by *Impulse Radio* based UWB signals. We have presented a methodology for construction of these codes and have shown that UWB signals employing these sequences have no impact on the achievable data-rate of 802.11a WLANs, even when operating in an NLOS environment. We also note that our design methodology is applicable to the mitigation of UWB interference on any narrowband system. The construction of this type codes can be extended to UWB systems using spread spread spectrum techniques.

References

[1] FCC, "Document 00-163: Revision of part 15 of the Commission's rules regarding Ultra-Wideband communications," *ET Docket No. 98-153*, April 2002.

[2] J. Foerster, E. Green, S. Somayazulu, and D. Leeper, "Ultra-Wideband technology for short- or medium-range wireless communications," *Intel Technology Journal*, Second Quarter, 2001.

[3] J. Bellorado, S.S. Ghassemzadeh, L.J. Greenstein, T. Sveinsson, and V. Tarokh, "Coexistence of Ultra-Wideband systems with IEEE-802.11a wireless LANs," in *IEEE Global Communications Conference (Globecom)*, (San Francisco, CA), 2003.

[4] J. Padgett, J. Koshy, and A. Triolo, "Physical-layer modeling of uwb interference effects," *http://www.darpa.mil/ato/solicit/NETEX/docs*, January 2003.

[5] IEEE, "Standard 802.11a: Part 11: Wireless LAN medium access control (MAC) and physical layer (PHY) specifications - High speed physical layer in the 5 GHz band," 1999.

[6] I. Bergel, E. Fishler, and H. Messer, "Narrow-band interference suppression in Impulse Radio," *submitted to IEEE Transactions on Communications*, 2002.

[7] L. Li and L. Milstein, "Rejection of narrow-band interference in pn spread spectrum systems using transversal filters," *IEEE Transactions on Communications*, vol. 30, no. 9, pp. 925–928, 1982.

[8] A. Taha and K. Chugg, "A theoretical study on the effects of interference on UWB multiple-access Impulse Radio," in *Asilomar Conference on Signals, Systems, and Computers*, 2002.

[9] IEEE, "Standard 802.15: Wireless Personal Area Network WPAN high rate alternative PHY task group 3a (TG3a)."

[10] M. Win and R. Scholtz, "Impulse radio: How it works," *IEEE Communication Letters*, vol. 2, January 1998.

[11] M. Win and R. Scholtz, "Ultra-wide bandwidth time-hopping spread-spectrum Impulse Radio for wireless multiple-access communications," *IEEE Transactions on Communications*, vol. 48, pp. 679–690, April 2000.

[12] J. Romme and L. Piazzo, "On the power spectral density of time-hopping Impulse Radio," in *IEEE Conference on Ultra Wideband Systems and Technologies (UWBST)*, (Baltimore, MD), 2002.

[13] H. Sheng, P. Orlik, A. M. Haimovich, L. Cimini, and Z. J., "On the spectral and power requirements for Ultra-Wideband transmission," in *IEEE International Conference on Communications*, (Anchorage, AK), 2003.

[14] T. Rappaport, *Wireless Communications, Principles and Practice*. Prentice Hall Inc., 1996.

[15] S.S Ghassemzadeh, R. Jana, C. Rice, W. Turin, and V. Tarokh, "A statistical path loss model for in-home UWB channels," in *IEEE Conference on Ultra-Wideband Systems and Technologies (UWBST)*, 2002.